

- cules, CA). After 24 hours, selection was initiated by addition of G418 (400 µg/ml) to the cell culture medium. A stable clone 9 cell line overexpressing GFP-Dyn2 was achieved within a month.
12. Clone 9 cells were maintained at 37°C in Ham's F-12K medium supplemented with 10% fetal bovine serum. Cells were grown on cover glasses for 1 to 3 days before microscopy.
  13. For immunolocalization, cells were fixed in aldehyde and then labeled as described (9) and mounted in ProLong antifade reagent (Molecular Probes, Eugene, OR). Alternatively, live cells were viewed directly. Either an epifluorescence microscope (Axiovert 35, Carl Zeiss) equipped with a 100-W mercury arc (attenuated up to 90%) and a cooled charged coupled device (CCD) camera (SenSys, Photometrics, Tucson, AR) or a confocal laser scanning microscope (LSM-410, Carl Zeiss) was used for fluorescence microscopy.
  14. The location of each peptide used as antigen within the dynamin molecule is shown in Fig. 3B. The Pan-dynamin MC63 antibody has been shown to specifically recognize a 100-kD dynamin band in rat liver fractions by immunoblotting and immunoprecipitation (9). The Pan-dynamin MC60 and Dyn2-specific antibodies also have been characterized (27). The antibodies added to cell-free assays were affinity purified and concentrated (~3 mg/ml); then they were tested by immunoblot analysis to confirm retention of activity (9). Antiserum against clathrin was produced from the hybridoma X22 (ATCC). The antibodies against the cytoplasmic and luminal domains of the plgA-R have been described (19). The rabbit polyclonal antibody to TGN38 was to a peptide representing the COOH-terminal cytoplasmic portion of the protein.
  15. K. Takei, P. S. McPherson, S. L. Schmid, P. De Camilli, *Nature* **374**, 186 (1995).
  16. S. M. Jones, K. E. Howell, J. R. Henley, H. Cao, M. A. McNiven, data not shown.
  17. R. S. Taylor, S. M. Jones, R. H. Dahl, M. H. Nordeen, K. E. Howell, *Mol. Biol. Cell* **8**, 1911 (1997).
  18. For the membrane binding assay, stacked Golgi fractions (SGF1) were isolated from rat liver (17). SGF1 (100 µg) plus cytosol (200 µg) were incubated in 25 mM Hepes (pH 6.7), 25 mM KCl, 1.5 mM magnesium acetate in a final volume of 1.0 ml at 37°C for 15 min. For assay mixtures that contained ATP, 1.0 mM ATP and an ATP regenerating system (8.0 mM creatine phosphate, 0.043 mg of creatine phosphokinase per milliliter) were added to the reaction mixture. For other assays GTP-γ-S was added to a final concentration of 10.0 µM. After incubation, the reaction mixture was loaded onto a 0.5 M sucrose cushion and centrifuged in a TL55 rotor at 55,000 rpm for 1 hour. Membrane pellets were resolved by SDS-PAGE, transferred to nitrocellulose filters, immunoblotted with antibodies against dynamin (MC63), which were detected with <sup>125</sup>I-labeled protein A (NEN, Boston, MA), and exposed to film for autoradiography. Immunoblots were quantitated with a PhosphorImager (Molecular Dynamics, Sunnyvale, CA).
  19. J. Salameo, E. S. Sztul, K. E. Howell, *Proc. Natl. Acad. Sci. U.S.A.* **87**, 7717 (1990).
  20. The cell-free assay of budding from immobilized stacked Golgi fractions was carried out as described (24). Each assay mixture contained a 2.5-mg magnetic core and shell beads with ~50 µg of the stacked Golgi fraction immobilized. The immobilized fraction has been characterized (24). For the budding reaction, the immobilized fraction was incubated in 2.5 ml containing cytosol at 0.70 mg/ml, 25 mM Hepes (pH 6.7), 25 mM KCl, 1.5 mM magnesium acetate, 1.0 mM ATP, an ATP regenerating system (8.0 mM creatine phosphate, 0.043 mg of creatine phosphokinase per milliliter), and 5 mg of bovine serum albumin (BSA) per milliliter (final concentrations). For cell-free assays in which antibodies were tested, increasing concentrations of antibody were incubated with the cytosol for 30 min on ice before addition to the cell-free assay. After 10 min at 37°C the Golgi fraction remaining on the beads was retrieved, and the budded vesicles remained in the supernatant. The budded fraction was pelleted through a 0.25 M sucrose cushion (100,000g for 1 hour) to deplete the BSA (5 mg/ml) and large amounts of cytosolic proteins. The pellet was resuspended in gel sample buffer and resolved by SDS-PAGE. Budding efficiency was reported as the percentage of the total mature sialylated plgA-R (116 kD) present in the budded fraction (100% represents the amount present in the immobilized SGF before budding). The plgA-R distribution was determined by quantitative immunoblotting of the fractions from the cell-free assay. Because the plgA-R is a plasma membrane receptor synthesized in relatively high amounts in rat liver (28), it defines a specific population of constitutive exocytic vesicles (24). The amount of clathrin-coated vesicle formation was assessed by determining the amount of clathrin heavy chain in the total budded vesicle fraction by quantitative immunoblotting with monoclonal antibody TD.1 (ATCC). Percentage budding was calculated as the amount of clathrin heavy chain in the pelleted total budded fraction compared with that found in control budding reactions (100%). The amount of clathrin-coated vesicle budding in the absence of ATP and cytosol was 3%.
  21. S. M. Jones, K. E. Howell, J. R. Henley, H. Cao, M. A. McNiven, data not shown.
  22. For depletion of dynamin proteins from rat liver cytosol, 2 ml of rat liver cytosol (16 mg/ml), prepared by the methods of Palade and coworkers (28), was passed repeatedly over an MC63 Pan-dynamin antibody column at 4°C. The cytosolic void volume next was passed repeatedly over a Dyn2-specific antibody column at 4°C. The void volume was concentrated, separated by SDS-PAGE, and immunoblotted with dynamin antibodies to confirm a complete depletion of dynamin proteins from the cytosol. The dynamin antibody columns were prepared by immobilizing 9.3 mg and 4.9 mg of affinity-purified MC63 or Dyn2-specific antibodies, respectively, per 1.5-ml column matrix. All antibodies were immobilized by using an Immunopure protein A IgG orientation kit (Pierce Chemical, Rockford, IL) according to the manufacturer's instructions.
  23. A dynamin-enriched fraction was isolated from freshly obtained rat brains according to established methods (9, 29). Briefly, a rat brain homogenate was passed through a 10-ml DEAE anion-exchange column and then added to a 5-ml phosphocellulose column. After substantial rinsing in 100 mM NaCl buffer, dynamin proteins were eluted from the column with 250 mM NaCl, and then the fractions were pooled, concentrated, dialyzed, and frozen in liquid nitrogen.
  24. S. M. Jones, R. H. Dahl, J. Ugelstad, K. E. Howell, in *Cell Biology: A Laboratory Handbook*, J. E. Celis, Ed. (Academic Press, London, ed. 2, 1997), vol. 2, pp. 12-25; M. Jones and K. E. Howell, *J. Cell Biol.* **139**, 339 (1997).
  25. R. B. Kelly, *Nature* **374**, 116 (1995); J. Roos and R. B. Kelly, *Trends Cell Biol.* **7**, 257 (1997).
  26. H. Cao and M. A. McNiven, unpublished work.
  27. J. R. Henley, E. W. A. Krueger, B. J. Oswald, M. A. McNiven, *J. Cell Biol.*, in press.
  28. E. S. Sztul, K. E. Howell, G. E. Palade, *ibid.* **100**, 1255 (1985).
  29. R. Scaife, I. Gout, M. D. Waterfield, R. L. Margolis, *EMBO J.* **13**, 2574 (1994).
  30. At UCHSC the use of the Hepatobiliary Center, Cell Biology Core (NIH, P30 DK-34914), and the Cancer Center Monoclonal Antibody Facility (P30 CA-46934) is acknowledged. We especially thank J. Ugelstad and R. Schmid, SINTEF, University of Trondheim, Norway, for the shell and core magnetic beads used in the cell-free assay. Thanks also goes to F. Garcia for her help with the GFP expression studies, to E. Krueger for his work on the GFP imaging, and to B. Oswald for help with preparation of antibodies and depleted cytosol.

12 September 1997; accepted 9 December 1997

## Gain-of-Function Mutations of *c-kit* in Human Gastrointestinal Stromal Tumors

Seiichi Hirota,\* Koji Isozaki,\* Yasuhiro Moriyama, Koji Hashimoto, Toshirou Nishida, Shingo Ishiguro, Kiyoshi Kawano, Masato Hanada, Akihiko Kurata, Masashi Takeda, Ghulam Muhammad Tunio, Yuji Matsuzawa, Yuzuru Kanakura, Yasuhisa Shinomura, Yukihiko Kitamura†

Gastrointestinal stromal tumors (GISTs) are the most common mesenchymal tumors in the human digestive tract, but their molecular etiology and cellular origin are unknown. Sequencing of *c-kit* complementary DNA, which encodes a proto-oncogenic receptor tyrosine kinase (KIT), from five GISTs revealed mutations in the region between the transmembrane and tyrosine kinase domains. All of the corresponding mutant KIT proteins were constitutively activated without the KIT ligand, stem cell factor (SCF). Stable transfection of the mutant *c-kit* complementary DNAs induced malignant transformation of Ba/F3 murine lymphoid cells, suggesting that the mutations contribute to tumor development. GISTs may originate from the interstitial cells of Cajal (ICCs) because the development of ICCs is dependent on the SCF-KIT interaction and because, like GISTs, these cells express both KIT and CD34.

The *c-kit* proto-oncogene encodes a type III receptor tyrosine kinase (KIT) (1), the ligand of which is SCF (2). SCF-KIT interaction is essential for development of melanocytes, erythrocytes, germ cells, mast cells and ICCs (3, 4). Gain-of-function mu-

tations of the *c-kit* gene have been found in several tumor mast cell lines of rodents and humans (5, 6) and in mast cell tumors of humans (7). Here we investigate the mutational status of *c-kit* in mesenchymal tumors of the human gastrointestinal (GI) tract.

We collected 58 mesenchymal tumors that developed in the GI wall (4 in the esophagus, 36 in the stomach, 14 in the small intestine, and 4 in the large intestine). KIT expression was examined by immunohistochemistry (8). Eight authentic leiomyomas and an authentic schwannoma did not express KIT. The remaining 49 mesenchymal tumors were diagnosed as gastrointestinal stromal tumors (GISTs), and 94% (46/49) of these expressed KIT. Examination of these tumors for expression of CD34, which is a reliable marker for GISTs (9), revealed that 82% (40/49) were CD34-positive, and 78% (38/49) were positive for both KIT and CD34 (Fig. 1, A to I). Three of five KIT-negative GISTs were also CD34-negative.

We compared the immunohistochemical characteristics of GISTs with those of ICCs, cells that regulate autonomous contraction of the GI tract (4). ICCs are located in and near the circular muscle layer of the stomach (10), small intestine (11), and large intestine (12). Because ICCs of the small intestine surrounding myenteric ganglion cells are easily identified by their specific localization, we examined the immunohistochemical characteristics of these cells and found that they were double-positive for KIT and CD34 (Fig. 2, A to G). ICCs in the circular muscle layer of the stomach and small intestine and ICCs in the myenteric plexus region and circular muscle layer of the large intestine were also double-positive for KIT and CD34.

We obtained the complete coding region of *c-kit* cDNA from six GISTs and control tissues using the reverse transcriptase-polymerase chain reaction (RT-PCR) (13). Ten independent *c-kit* clones were obtained from each sample. In 5 of the 6 GISTs (GIST 1 to 5), 4 to 6 clones out of 10 examined showed mutations in the region between the transmembrane and tyrosine kinase domains (hereafter called juxtamembrane domain) (Fig. 3). These mutations were located within an 11-amino acid

stretch (Lys-550 to Val-560), but at nonidentical sites. No mutations were detectable in other domains of *c-kit* cDNA. Because ~50% of the cDNA clones from each GIST did not show any mutations, we conclude that only one of the two *c-kit* alleles was mutated in each case. Direct sequencing of the PCR products confirmed the mutations in the jux-

tamembrane domain of *c-kit* cDNA in the five GISTs.

We next examined whether the *c-kit* mutations found in the GISTs resulted in constitutive activation of the *c-kit* receptor tyrosine kinase by transient introduction of the mutant *c-kit* cDNAs into the 293T human embryonic kidney (HEK) cell line (5, 14,

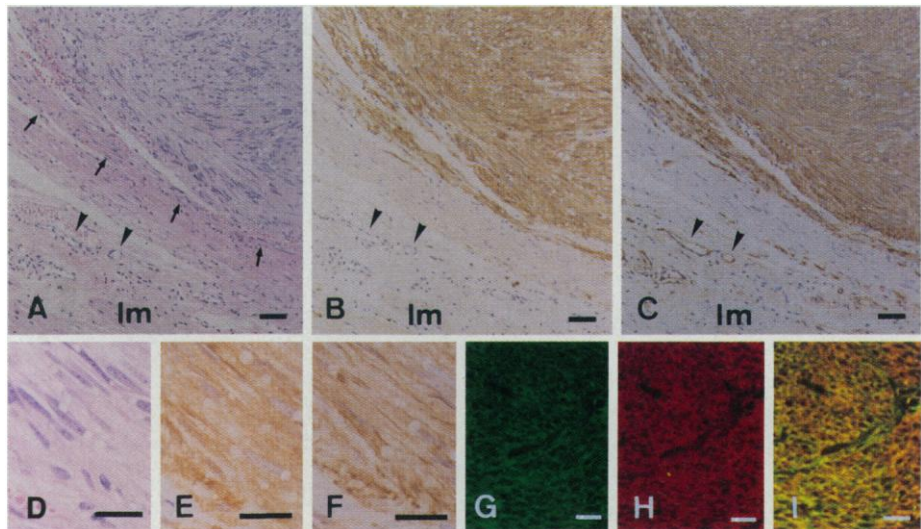


**Fig. 1.** Coexpression of KIT and CD34 in human GISTs. (A to C) Serial sections of a tumor that developed in the muscle layers of the stomach. (D to F) Higher magnification of (A) to (C). (A) and (D) are stained with hematoxylin and eosin. The boundary of the tumor is indicated by arrows in (A). (B) and (E) are stained with anti-KIT and (C) and (F) with anti-CD34 (8). Arrowheads in (A) to (C) indicate that endothelial cells of blood vessels express CD34 but not KIT. Im; longitudinal muscle layer. (G to I) Coexpression of KIT and CD34 in another GIST, also from the stomach, demonstrated by confocal laser scanning microscopy (8). (G) Binding of rabbit anti-KIT to tumor cells demonstrated by FITC-labeled anti-rabbit IgG (green). (H) Binding of mouse anti-CD34 to tumor cells demonstrated by RPE-labeled anti-mouse IgG (red). (I) Merged confocal image of (G) and (H) showing coexpression of KIT and CD34 in tumor cells (yellow). Bars in (A) to (C), 50  $\mu$ m; in (D) to (I), 100  $\mu$ m.

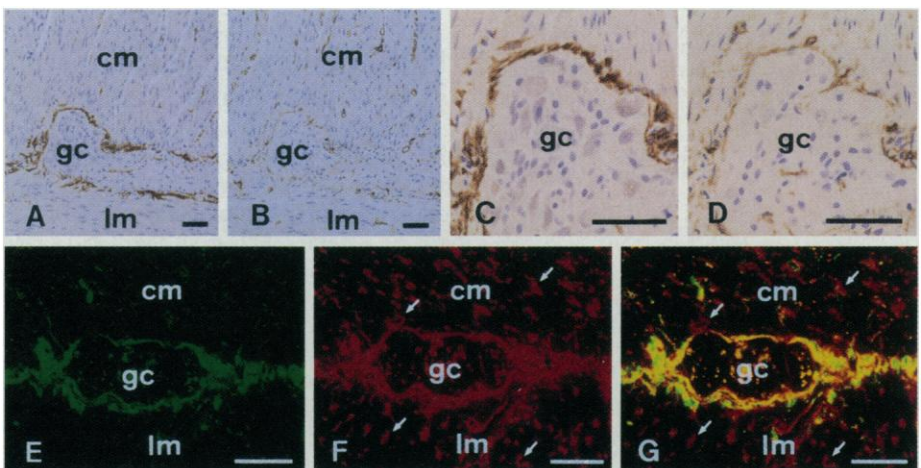


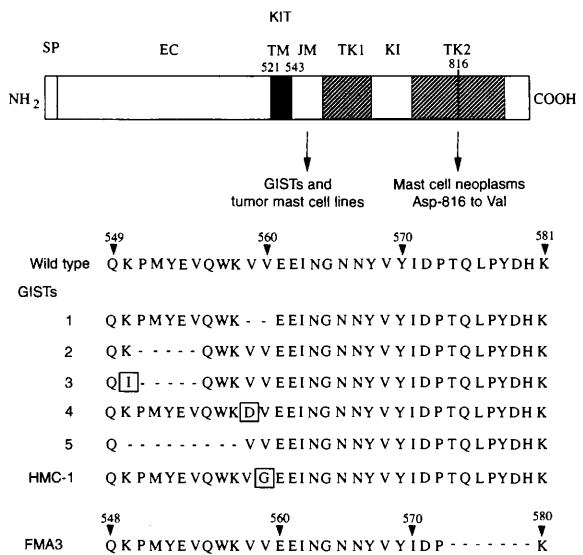
**Fig. 2.** Coexpression of KIT and CD34 in ICCs surrounding myenteric ganglion cells in normal human small intestine. (A and B) Serial sections of the normal human small intestine. (C and D) Higher magnification of (A) and (B), respectively. (A) and (C) are stained with anti-KIT and (B) and (D) are stained with anti-CD34 (8). The localization of KIT and CD34 double-positive cells is consistent with that of ICCs, which are present between the circular muscle layer (cm) and the longitudinal muscle layer (lm), and surrounding the myenteric ganglion cells (gc) (11). (E to G) Demonstration by confocal laser scanning microscopy (8). (E) Binding of rabbit anti-KIT. (F) Binding of mouse anti-CD34. (G) Merged confocal image of (E) and (F). Arrows in (F) and (G) show endothelial cells and fibroblast-like cells that express CD34 but not KIT. Bars in (A) to (G), 50  $\mu$ m.

S. Hirota, K. Hashimoto, G. M. Tunio, Y. Kitamura, Department of Pathology, Osaka University Medical School, Yamada-oka 2-2, Suita 565, Japan.  
K. Isozaki, Y. Moriyama, Y. Matsuzawa, Y. Shinomura, Department of Internal Medicine II, Osaka University Medical School, Yamada-oka 2-2, Suita 565, Japan.  
T. Nishida, Department of Surgery I, Osaka University Medical School, Yamada-oka 2-2, Suita 565, Japan.  
S. Ishiguro, Division of Pathology, Osaka Medical Center for Cancer and Cardiovascular Diseases, Osaka, Japan.  
K. Kawano, Division of Pathology, Osaka Rosai Hospital, Sakai, Japan.  
M. Hanada, Division of Pathology, Toyonaka Municipal Hospital, Toyonaka, Japan.  
A. Kurata and M. Takeda, Division of Pathology, Osaka National Hospital, Osaka, Japan.  
Y. Kanakura, Department of Hematology/Oncology, Osaka University Medical School, Yamada-oka 2-2, Suita 565, Japan.

\*These authors contributed equally to this work.  
†To whom correspondence should be addressed. E-mail: kitamura@patho.med.osaka-u.ac.jp

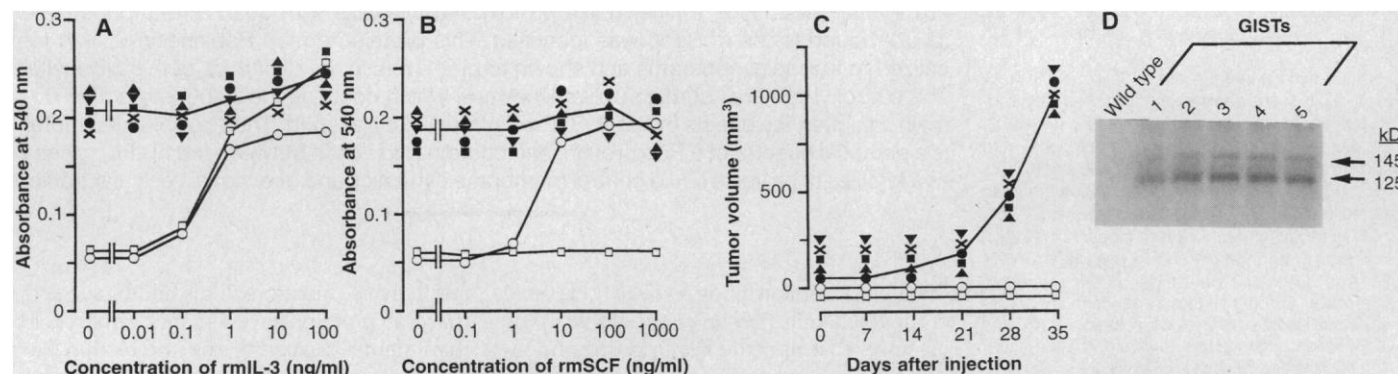
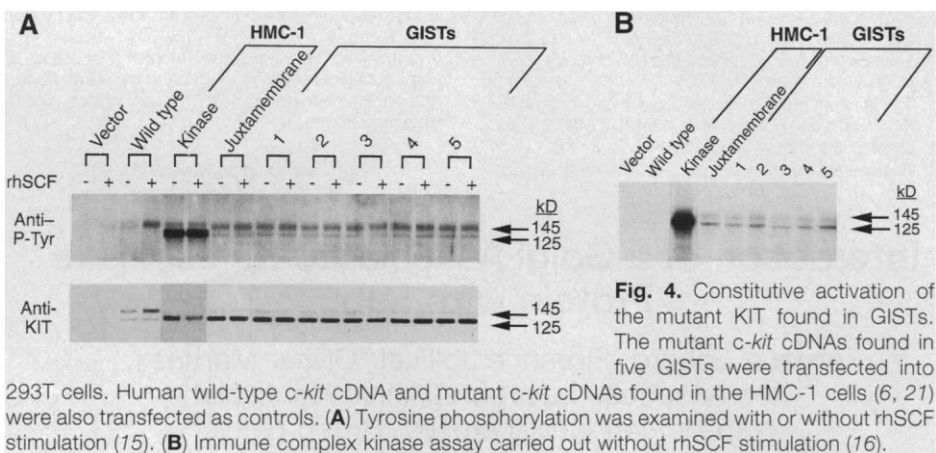
**Fig. 3.** Mutations of *c-kit* in GISTs.

GIST 1 showed an in-frame deletion of 6 base pairs (bp). GIST 2 showed an in-frame deletion of 15 bp. GIST 3 showed the same in-frame deletion as observed in GIST 2 and an additional point mutation at codon 550 (AAA to ATA) that resulted in a Lys<sup>550</sup>→Ile substitution. GIST 4 showed a point mutation at codon 559 (GTT to GAT) that resulted in a Val<sup>559</sup>→Asp substitution. GIST 5 showed an in-frame deletion of 27 bp. The *c-kit* mutations in the juxtamembrane domain of the HMC-1 human mast cell leukemia cell line (5) and the FMA3 murine mastocytoma cell line (6) are shown for comparison. Deleted amino acids are shown by dashes (-) and mutated amino acids by boxes. Murine and human KIT are of different lengths (7), so the amino acid numbering in the FMA3 KIT is different. Abbreviations used are as follows: SP, signal peptide; EC, extracellular domain; TM, transmembrane domain; JM, juxtamembrane domain; TK1 and TK2, tyrosine kinase domains; and KI, kinase insert. Abbreviations for the amino acid residues are as follows: D, Asp; E, Glu; G, Gly; H, His; I, Ile; K, Lys; L, Leu; M, Met; N, Asn; P, Pro; Q, Gln; T, Thr; V, Val; W, Trp; and Y, Tyr.



15). The wild-type *c-kit* cDNA was introduced as a negative control, and the tyrosine kinase domain mutant and the juxtamembrane domain mutant found in the HMC-1 human mast cell leukemia cell line (5) were introduced as positive controls. Wild-type KIT was phosphorylated on tyrosine only when recombinant human (rh) SCF was added to the culture medium (Fig. 4A). In contrast, the gain-of-function KIT mutants found in HMC-1 cells were phosphorylated on tyrosine without the addition of rhSCF, as reported previously (5). The magnitude of the constitutive tyrosine phosphorylation was greater in the tyrosine kinase domain mutant than in the juxtamembrane domain mutant. The *c-kit* mutants found in GISTs also showed the constitutive tyrosine phosphorylation in 293T cells without rhSCF (Fig. 4A). The constitutive tyrosine phosphorylation of the juxtamembrane mutant of HMC-1 cells was of similar magnitude to that of the juxtamembrane mutants of GISTs. In vitro kinase assays (16), the *c-kit* mutants found in the GISTs exhibited constitutive kinase activation that was similar in magnitude to that of the juxtamembrane domain mutant of HMC-1 cells (5) (Fig. 4B).

To investigate the biological consequences of the mutant *c-kit*, we introduced the *c-kit* mutations found in the GISTs into the mouse *c-kit* cDNA (17) and then stably transfected the cDNA into the interleukin 3 (IL-3)-dependent Ba/F3 murine lymphoid cell line (18). As a control, mouse wild-type *c-kit* cDNA was also transfected into Ba/F3 cells. We estimated Ba/F3 cell proliferation using an MTT colorimetric assay (19). Ba/F3 cells with the wild-type murine *c-kit* grew in the presence of either recombinant mouse (rm) IL-3 or rmSCF; Ba/F3 cells with the mutated murine *c-kit* grew autonomously without rmIL-3 and rmSCF (Fig. 5, A and B). Ba/F3 cells with the mutated murine *c-kit* also grew autonomously in nude mice (Fig.



5C) (20). The constitutive kinase activation of all KIT mutants found in the five GISTs was confirmed in Ba/F3 cells (Fig. 5D) (5, 21).

Although various cells including hematopoietic stem cells express both KIT and CD34 (22), ICCs are the only cells that are double-positive for KIT and CD34 in normal GI wall of humans. This strongly suggests that KIT and CD34 double-positive GISTs might originate from ICCs, although we cannot exclude the possibility that ICCs and GISTs simply show common undifferentiated characteristics such as those observed in multipotential hematopoietic stem cells.

The mechanism by which KIT becomes constitutively activated appears to be different for the tyrosine kinase domain mutant and the juxtamembrane domain mutant (6, 21). The former is constitutively activated without forming dimers (21), whereas the latter constitutively dimerizes without binding SCF (6, 21). The tyrosine kinase domain mutation of KIT has been found only in mast cell neoplasms (7) and its juxtamembrane domain mutation only in GISTs. The mechanisms by which these different mutations cause malignant transformation of different cell types remain to be investigated.

## REFERENCES AND NOTES

1. P. Besmer *et al.*, *Nature* **320**, 415 (1986); B. Chabot, D. A. Stephenson, V. M. Chapman, P. Besmer, A. Bernstein, *ibid.* **335**, 88 (1988); E. N. Geissler, M. A. Ryan, D. E. Houseman, *Cell* **55**, 185 (1988).
2. D. E. Williams *et al.*, *Cell* **63**, 167 (1990); J. G. Flanagan and P. Leder, *ibid.*, p. 185; K. M. Zsebo *et al.*, *ibid.*, p. 213; E. Huang *et al.*, *ibid.*, p. 225.
3. E. S. Russel, *Adv. Genet.* **20**, 357 (1979); Y. Kitamura, S. Go, K. Hatanaka, *Blood* **52**, 447 (1978); Y. Kitamura and S. Go, *ibid.* **53**, 492 (1979).
4. H. Maeda *et al.*, *Development* **116**, 369 (1992); J. D. Huizinga *et al.*, *Nature* **373**, 347 (1995); K. Isozaki *et al.*, *Gastroenterology* **109**, 456 (1995).
5. T. Furitsu *et al.*, *J. Clin. Invest.* **92**, 1736 (1993).
6. T. Tsujimura *et al.*, *Blood* **83**, 2619 (1994); T. Tsujimura *et al.*, *Int. Arch. Allergy Immunol.* **106**, 377 (1995); T. Tsujimura *et al.*, *Blood* **87**, 273 (1996).
7. H. Nagata *et al.*, *Proc. Natl. Acad. Sci. U.S.A.* **92**, 10560 (1995); B. J. Longley *et al.*, *Nature Genet.* **12**, 312 (1996).
8. Formalin-fixed paraffin sections (3  $\mu$ m thick) were used (23). For enzyme immunohistochemistry, rabbit polyclonal antibody against human KIT (K963; IBL, Fujioka, Japan) and mouse monoclonal antibody (mAb) against human CD34 (QBend10; Novocastra laboratories, Newcastle, UK) were used as the primary antibodies. Biotinylated goat antibody to rabbit (anti-rabbit) immunoglobulin G (IgG) and biotinylated rabbit anti-mouse IgG (DAKO; Glostrup, Denmark) were used as the secondary antibodies. Binding of the secondary antibodies was visualized as in (23). Coexpression of KIT and CD34 was confirmed with a confocal laser scanning microscope (Olympus LSM-GB200; Olympus, Tokyo, Japan). Fluorescein isothiocyanate (FITC)-conjugated swine anti-rabbit IgG and R-phycoerythrin (RPE)-conjugated goat anti-mouse IgG (DAKO) were used as the secondary antibodies. The excitation wavelength is 488 nm for FITC and 515 nm for RPE.
9. M. van de Rijn, M. R. Hendrickson, R. V. Rouse,

- Hum. Pathol.* **25**, 776 (1994); J. M. Monihan, N. J. Carr, L. H. Sobin, *Histopathology* **25**, 469 (1994); M. Miettinen, M. Virolainen, M. S. Rikala, *Am. J. Surg. Pathol.* **19**, 207 (1995).
10. M. S. Fausone-Pellegrini, D. Panthalone, C. Cortesini, *J. Submicrosc. Cytol. Pathol.* **21**, 439 (1987); J.-M. Vanderwinden, H. Liu, M.-H. D. Laet, J.-J. Vanderhaeghen, *Gastroenterology* **111**, 279 (1996).
11. R. Matsuda *et al.*, *Am. J. Pathol.* **142**, 339 (1993); J.-M. Vanderwinden *et al.*, *Gastroenterology* **111**, 901 (1996); J. J. Rumessen, H. B. Mikkelsen, L. Thuneberg, *ibid.* **102**, 56 (1992); J. J. Rumessen, H. B. Mikkelsen, K. Qvortrup, L. Thuneberg, *ibid.* **104**, 343 (1993).
12. M. S. Fausone-Pellegrini, C. Cortesini, D. Panthalone, *Can. J. Physiol. Pharmacol.* **68**, 1437 (1990); J. J. Rumessen, S. Peters, L. Thuneberg, *Lab. Invest.* **68**, 481 (1993).
13. From 10  $\mu$ g of total RNA, cDNA was synthesized and amplified as in (24). Oligonucleotide primer sets used were as described (5). The cDNAs were sequenced directly or after subcloning into Bluescript I KS(-) by Model 373A DNA sequencer (Applied Biosystems, Foster City, CA).
14. The coding region of the human wild-type *c-kit* was cloned into Xba I site of expression vector pEF-BOS. The Sna BI-Mro I fragment (nucleotide 1141 to 2282) of the human wild-type *c-kit* in the expression vector was replaced by the corresponding fragments of the mutant-type cDNA obtained from each GIST. The expression vectors were transfected into the 293T HEK cell line by calcium phosphate precipitation (5).
15. The procedures of cell lysis, immunoprecipitation, SDS-polyacrylamide gel electrophoresis, and immunoblotting were done as in (5). Mouse mAb to human KIT (MCA955; Serotec, Oxford, UK) was used for the immunoprecipitation. Immunoblotting was done with mouse mAb to phosphotyrosine (4G10; Upstate Biotechnology, Lake Placid, NY) or rabbit polyclonal anti-human KIT (K963).
16. The immune complex kinase assay was done as in (5). Rabbit polyclonal anti-human KIT (K963) was used for the immunoprecipitation.
17. To generate the murine-type *c-kit* cDNAs containing

the same mutation as the GISTs, we performed site-directed mutagenesis (5). The Nde I-Spl I fragment with the mutation was isolated and inserted into the expression vector pEF-BOS containing murine wild-type *c-kit* cDNA.

18. A Sca I-cut expression vector pEF-BOS containing the mouse-type mutated *c-kit* cDNA and the Bam HI-cut expression vector pSV2-neo were cotransfected into the IL-3-dependent Ba/F3 murine lymphoid cell line with the use of GENE PULSER II (Bio-Rad Laboratories). After transfection, the cells expressing neomycin-resistant gene were selected by cultivation in medium containing G418 (0.6 mg/ml) and rmlL-3 for 4 weeks. Cloning of the cells was done with the limiting-dilution method, and the expression of each mutated *c-kit* was confirmed by flow cytometry, protein immunoblotting, and RT-PCR with sequencing.
19. To quantitate cell proliferation, we used the MTT [3-(4,5-dimethylthiazol-2-yl)-2,5-diphenyl tetrazolium bromide] (Sigma) rapid colorimetric assay. The procedure was done as in (6).
20. Cells ( $10^7$ ) were transplanted subcutaneously at the posterior flank of nude mice. Untransfected Ba/F3 cells and Ba/F3 cells expressing the murine wild-type KIT were used as controls. Tumors were measured with the vernier caliper every 4 days. The tumor volume ( $V$ ) was calculated with the formula  $V = 0.5 \times a \times b^2$ , where  $a$  and  $b$  are the length and width in millimeters of the tumor mass, respectively.
21. H. Kitayama *et al.*, *Blood* **85**, 790 (1995).
22. L. K. Ashman, A. C. Cambareri, L. B. To, R. J. Levinsky, C. A. Juttner, *ibid.* **78**, 30 (1991); J. P. Catlett, J. A. Leftwich, E. H. Westin, S. Grant, T. F. Huff, *ibid.*, p. 3186.
23. S. Hirota *et al.*, *Lab. Invest.* **72**, 64 (1995).
24. S. Hirota *et al.*, *Arch. Pathol. Lab. Med.* **117**, 996 (1993).
25. We thank A. Fukuyama and K. Morihana for preparing histological sections. Supported by grants from the Japanese Ministry of Education, Science, Culture, and Sports.

13 May 1997; accepted 25 November 1997

## Interaction of a Golgi-Associated Kinesin-Like Protein with Rab6

Arnaud Echard, Florence Jollivet, Olivier Martinez, Jean-Jacques Lacapère, Annie Rousselet, Isabelle Janoueix-Lerosey, Bruno Goud\*

Rab guanosine triphosphatases regulate vesicular transport and membrane traffic within eukaryotic cells. Here, a kinesin-like protein that interacts with guanosine triphosphate (GTP)-bound forms of Rab6 was identified. This protein, termed Rabkinesin-6, was localized to the Golgi apparatus and shown to play a role in the dynamics of this organelle. The carboxyl-terminal domain of Rabkinesin-6, which contains the Rab6-interacting domain, inhibited the effects of Rab6-GTP on intracellular transport. Thus, a molecular motor is a potential effector of a Rab protein, and coordinated action between members of these two families of proteins could control membrane dynamics and directional vesicular traffic.

Small guanosine triphosphatases (GTPases) of the Rab family play an essential role in the processes that underlie the targeting and fusion of transport vesicles with their appropriate acceptor membrane (1). Within the past few years, several putative effectors that interact with Rab proteins in their GTP-bound conformation have been identified (2). They are not related to each other and appear to

fulfill diverse functions. This finding suggests that Rab proteins have a more complex role than simply regulating the interaction between proteins involved in the recognition of transport vesicles with membranes (3). On the other hand, it is now well established that intracellular organelles and vesicles, including the endoplasmic reticulum (ER) and Golgi membranes, move along cytoskeletal